Supporting Information

BTZ-derived benzisothiazolinones with *in vitro* activity against *Mycobacterium tuberculosis*

Adrian Richter[a], Rüdiger W. Seidel[a], Richard Goddard[b], Tamira Eckhardt[a], Christoph Lehmann[a], Julia Dörner[a], Fabienne Siersleben,[a] Theresia Sondermann,[a] Lea Mann,[a] Michael Patzer,[b] Christian Jäger[c], Norbert Reiling[d,e], Peter Imming[a]*

[a] Martin-Luther-Universität Halle-Wittenberg, Wolfgang-Langenbeck-Str. 4, 06120 Halle (Saale), Germany

[b] Max-Planck-Institut für Kohlenforschung, Kaiser-Wilhelm-Platz 1, 45470 Mülheim an der Ruhr, Germany

[c] Fraunhofer-Institut für Zelltherapie und Immunologie, Außenstelle Molekulare Wirkstoffbiochemie und Therapieentwicklung, Weinbergweg 22, 06120 Halle (Saale), Germany

[d] Microbial Interface Biology, Research Center Borstel, Leibniz Lung Center, Borstel, Germany

[e] German Center for Infection Research (DZIF), Site Hamburg-Lübeck-Borstel-Riems, Borstel, Germany

* Corresponding author: peter.imming@pharmazie.uni-halle.de

Table of Contents

Experimental section

Supporting figures

Supporting tables

1. General

Starting materials were purchased and used as received. Solvents were distilled prior to use and stored over 4 Å molecular sieves. Flash chromatography was performed on a puriFlash® 430 instrument (Interchim, Montluçon, France). Columns with silica gel (40-63 µm) were used. Column chromatography was carried out using Merck silica gel 60 (63-200 µm). The maximum compound load per column was 5 % (m/m) of the silica gel quantity.

NMR spectra were recorded on an Agilent Technologies VNMRS 400 MHz spectrometer. Chemical shifts are reported relative to the residual solvent signal of chloroform-*d* (δ_H = 7.26 ppm; δ_C = 77.10 ppm). Abbreviations: s = singlet, d = doublet, dd = doublet of doublets, m = multiplet, q = quartet. High-resolution mass spectra (HRMS) were recorded on a Thermo Fisher Scientific LTQ Orbitrap XL mass spectrometer. HPLC analyses were performed using an Agilent 1260 HPLC instrument equipped with UV diode array detection (50 mm Eclipse Plus C18 1.8 µm, 4.6 mm, methanol/water gradient, v = 1.0 mL min^{-1}, λ = 220 nm).

For the experiments described no unexpected or unusually high safety hazards were encountered.

2. Synthesis

2.1 7-nitro-5-(trifluoromethyl)benzo[d]isothiazol-3(2H)-one (**3**)

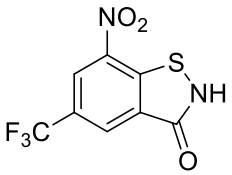

3

A suspension of CuI and 1,10-phenanthroline was stirred under argon atmosphere for 15 min in a 50 mL flask. 2-chloro-5-trifluoromethyl-3-nitrobenzamide,[1] sulfur and K_2CO_3 were added and the reaction was stirred for 15 min at room temperature. After heating at 110 °C overnight 56 mL brine were added and the reaction was stirred for 3 hours followed by extraction with ethyl acetate (3 × 60 mL). The combined organic layers were dried over Na_2SO_4 and the solvent was removed under reduced pressure. The product was isolated by flash chromatography (heptane/ethyl acetate gradient + 1% formic acid) as a yellow solid (2.39 g, 32%). ^{1}H NMR (400 MHz, chloroform-*d*): δ 8.81 (s, 1H), 8.67 (s, 1H) ppm.

*2.2 7-nitro-2-(piperidine-1-carbonyl)-5-(trifluoromethyl)benzo[d]isothiazol-3(2H)-one (**4a**) and 7-nitro-5-(trifluoromethyl)benzo[d]isothiazol-3-yl piperidine-1-carboxylate (**5a**)*

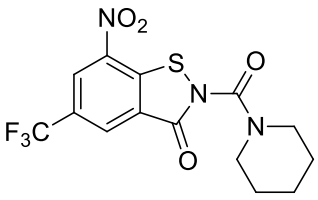

4a

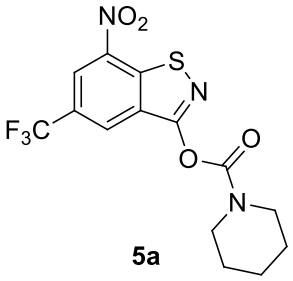

5a

Piperidine-1-carbonyl chloride (0.084 mL, 0.83 mmol) and **3** (110 mg, 0.42 mmol) were dissolved in 5 mL of dichloromethane and pyridine (0.668 mL, 8.3 mmol) was added. The reaction mixture was stirred for 24 hours at room temperature. Separation of **4a** and **5a** was carried out by flash chromatography (heptane/ethyl acetate gradient) followed by column chromatography eluting with dichloromethane.

7-nitro-2-(piperidine-1-carbonyl)-5-(trifluoromethyl)benzo[d]isothiazol-3(2H)-one (**4a**): Compound **4a** was isolated as a yellow solid (41 mg, 26 %, HPLC purity 93.8 %, t_R = 13.8 min). ^{1}H NMR (500 MHz, chloroform-*d*): δ 8.77 (d, ^4J = 1.6 Hz, 1H), 8.57 (d, ^4J = 1.6 Hz, 1H), 3.57 (m, 4H), 1.76–1.70 (m, 6H) ppm. ^{13}C NMR (126 MHz, chloroform-*d*) δ 161.0, 149.5, 142.3, 140.4, 130.4 (q, $^3J_{C,F}$ = 3.6 Hz), 129.8 (q, $^2J_{C,F}$ = 35.3 Hz), 128.5, 125.5 (q, $^3J_{C,F}$ = 3.6 Hz), 123.7 (q, $^1J_{C,F}$ = 273.7 Hz), 48.0, 25.9, 24.2 ppm. HRMS(ESI): *m*/*z* calcd. for $C_{14}H_{13}F_3N_3O_4S^+$ $[M+H]^+$, 376.0573; found, 376.0573.

7-nitro-5-(trifluoromethyl)benzo[d]isothiazol-3-yl piperidine-1-carboxylate (**5a**): Compound **5a** was isolated as a beige solid (86 mg, 54 %, HPLC purity 98.6 %, t_R = 14.9 min). ^{1}H NMR (500 MHz, chloroform-*d*): δ 8.72 (s, 1H), 8.43 (s, 1H), 3.78–3.69 (m, 2H), 3.62–3.55 (m, 2H), 1.82–1.63 (m, 6H). ^{13}C NMR (126 MHz, chloroform-*d*): δ 157.4, 150.9, 149.4, 141.4, 130.2, 129.3 (q, $^2J_{C,F}$ = 34.8 Hz), 127.0 (q, $^3J_{C,F}$ = 3.9 Hz), 123.9 (q, $^3J_{C,F}$ = 273.2 Hz), 121.8 (q, $^3J_{C,F}$ = 3.4 Hz), 46.4, 45.9, 26.0, 25.5, 24.2 ppm. HRMS(ESI): *m*/*z* calcd. for $C_{14}H_{13}F_3N_3O_4S^+$ $[M+H]^+$, 376.0573; found, 376.0572.

2.3 (S)-2-methyl-1,4-dioxa-8-azaspiro[4.5]decane-8-carbonyl chloride

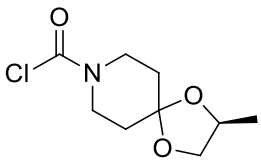

A two-neck flask was purged thrice with argon. Triphosgene (520 mg, 1.75 mmol) and dichloromethane (10 mL) were added and the mixture was cooled to 0 °C before pyridine (1.0

mL) was added. After stirring for 15 min at 0 °C, (*S*)-2-methyl-1,4-dioxa-8-azaspiro[4.5]decane (550 mg, 3.5 mmol) was slowly added to the mixture. After warming to room temperature, the reaction was stirred for 6 hours and then carefully quenched by 1 N HCl, followed by extraction with dichloromethane (3 × 20 mL). The combined organic layers were washed with water and brine and then dried over Na_2SO_4. The solvent was removed under reduced pressure and the product was isolated by flash chromatography (ethyl acetate/heptane 1:1) to yield *(S)*-2-methyl-1,4-dioxa-8-azaspiro[4.5]decane-8-carbonyl chloride as a colourless oil (398 mg, 52 %). ^{1}H NMR (400 MHz, chloroform-*d*): δ 4.31–4.18 (m, 1H), 4.07 (dd, ^2J = 7.9 Hz, ^3J = 5.7 Hz, 1H), 3.88–3.59 (m, 4H), 3.46 (t, ^2J = 7.9 Hz, 1H), 1.83–1.67 (m, 4H), 1.28 (d, ^3J = 6.1 Hz, 3H). ^{13}C NMR (101 MHz, chloroform-*d*): δ 148.1, 106.5, 72.3, 70.8, 46.9, 46.8, 44.3, 44.3, 36.5, 36.0, 35.3, 34.8, 18.4 ppm.

*2.4 (S)-2-(2-methyl-1,4-dioxa-8-azaspiro[4.5]decane-8-carbonyl)-7-nitro-5-(trifluoromethyl) benzo[d]isothiazol-3(2H)-one (**4b**) and 7-nitro-5-(trifluoromethyl) benzo[d]isothiazol-3-yl (S)-2-methyl-1,4-dioxa-8-azaspiro[4.5] decane-8-carboxylate (**5b**)*

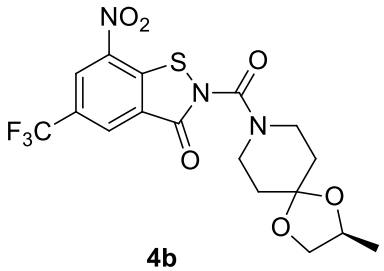

4b

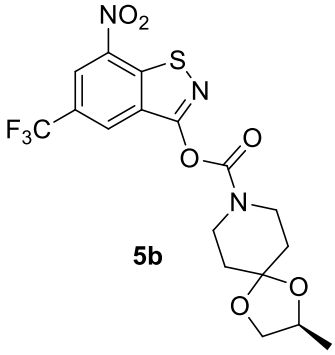

5b

(*S*)-2-methyl-1,4-dioxa-8-azaspiro[4.5]decane-8-carbonyl chloride (360 mg; 1.6 mmmol) and 3 (264 mg, 1.0 mmol) were dissolved in 10 mL of dichloromethane and pyridine (1.32 mL, 16.4 mmol) was added. The reaction mixture was stirred for 24 hours at room temperature. Purification was carried out by flash chromatography (heptane/ethyl acetate gradient).

(S)-2-(2-methyl-1,4-dioxa-8-azaspiro[4.5]decane-8-carbonyl)-7-nitro-5-(trifluoromethyl) benzo[d]isothiazol-3(2H)-one (**4b**): Compound **4b** was isolated as a yellow solid (122 mg, 27%, HPLC purity 96.9 %, t_R = 13.8 min). ^{1}H NMR (400 MHz, chloroform-*d*): δ 8.76 (s, 1H), 8.57 (s, 1H), 4.33–4.22 (m, 1H), 4.10 (dd, ^2J = 8.0 Hz, ^3J = 5.7 Hz, 1H), 3.78–3.62 (m, 4H), 3.49 (t, ^2J = 7.9 Hz, 1H), 1.96–1.82 (m, 4H), 1.30 (d, ^3J = 6.0 Hz, 3H). ^{13}C NMR (101 MHz, chloroform-*d*): δ 160.9, 149.5, 142.1, 140.3, 130.3 (q, $^3J_{C,F}$ = 3.5 Hz), 129.7 (q, $^2J_{C,F}$ = 35.4 Hz),

128.3, 125.5 (q, $^{3}J_{C,F}$ = 3.6 Hz), 122.4 (q, $^{1}J_{C,F}$ = 273.0 Hz), 106.6, 72.3, 70.8, 44.9, 36.2, 35.0, 18.4. HRMS *m*/*z* calcd. for $C_{17}H_{17}F_3N_3O_6S^+$ $[M+H]^+$, 448.0785; found, 448.0784.

7-nitro-5-(trifluoromethyl)benzo[d]isothiazol-3-yl (S)-2-methyl-1,4-dioxa-8-azaspiro[4.5] decane-8-carboxylate (**5b**): Compound **5b** was isolated as a pale yellow solid (248 mg, 55 %, HPLC purity 98.2 %, t_R = 14.2 min). ^{1}H NMR (400 MHz, chloroform-*d*): δ 8.73 (d, ^{4}J = 1.4 Hz, 1H), 8.42 (d, ^{4}J = 1.5 Hz, 1H), 4.33–4.25 (m, 1H), 4.12 (dd, ^{2}J = 7.9 Hz, ^{3}J = 5.7 Hz, 1H), 3.91–3.66 (m, 4H), 3.51 (td, ^{2}J = 7.9 Hz, ^{3}J = 1.8 Hz, 1H), 1.93–1.78 (m, 4H), 1.32 (d, ^{3}J = 6.0 Hz, 3H) ppm. ^{13}C NMR (126 MHz, chloroform-*d*): δ 157.6, 151.2, 149.8, 141.8, 130.5, 129.8 (q, $^{2}J_{C,F}$ = 34.7 Hz), 127.4 (q, $^{3}J_{C,F}$ = 3.8 Hz), 124.3 (q, $^{1}J_{C,F}$ = 274:2 Hz), 122.3 (q, $^{3}J_{C,F}$ = 3.4 Hz), 107.0, 72.9, 72.9, 71.4, 44.0, 43.9, 43.6, 43.5, 37.0, 36.5, 35.9, 35.3, 19.0 ppm. HRMS(ESI) *m*/*z* calcd. for $C_{17}H_{17}F_3N_3O_6S^+$ $[M+H]^+$, 448.0785; found, 448.0783.

3. NMR spectra und HPLC traces

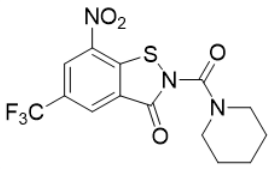

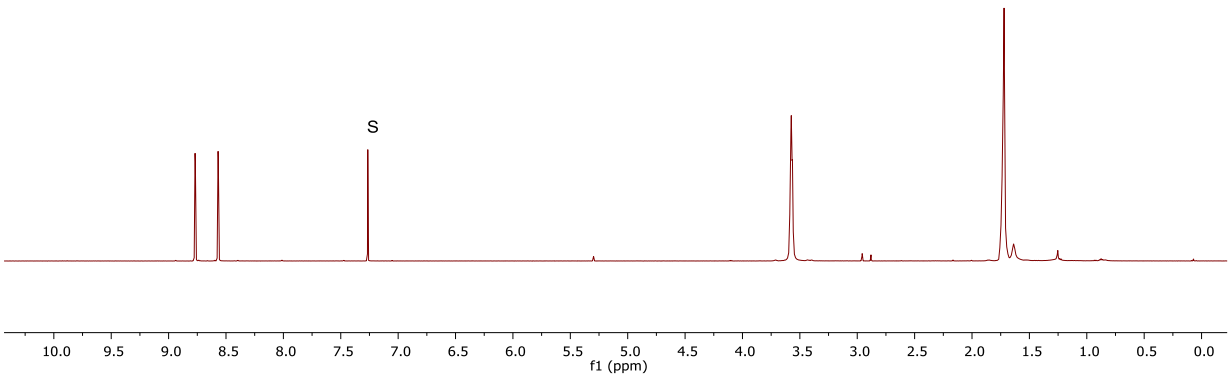

Figure S1 ^{1}H NMR spectrum (500 MHz, chloroform-*d*) of **4a**.

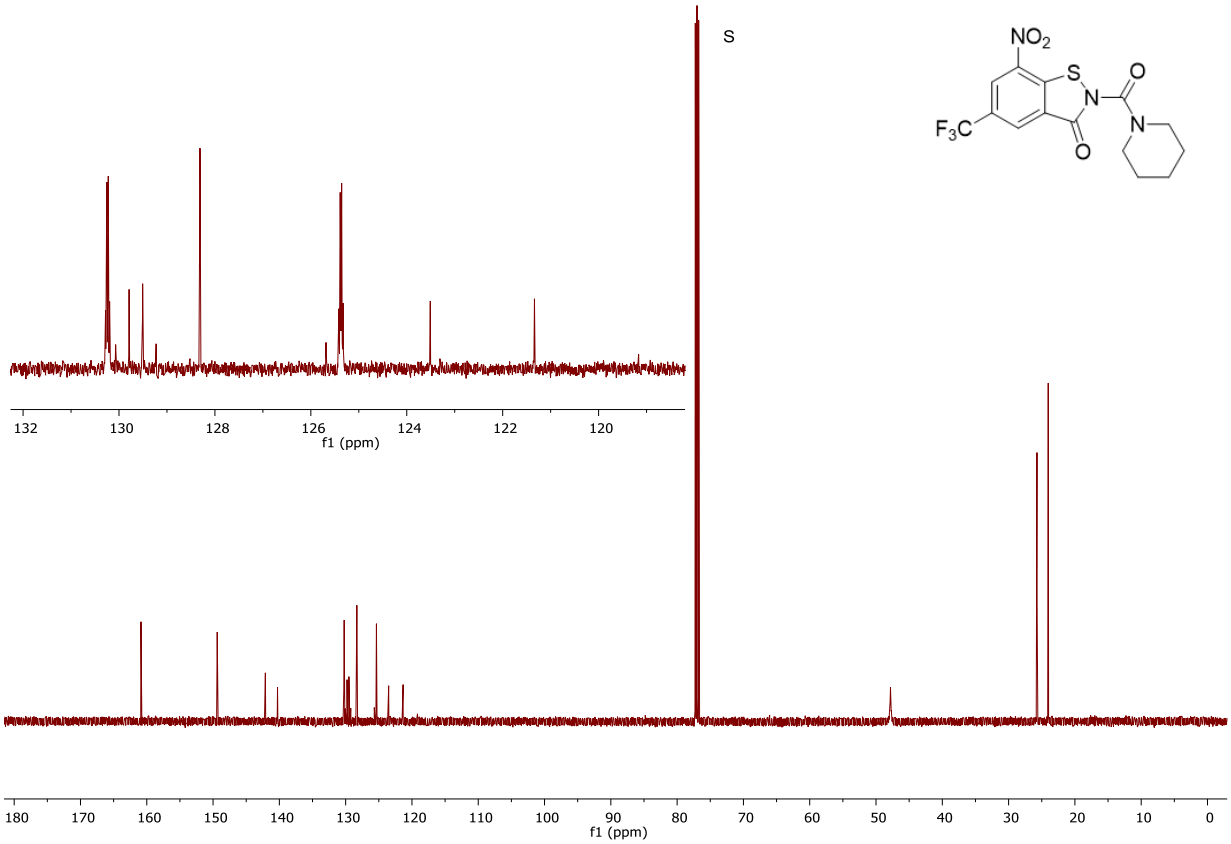

Figure S2 ^{13}C NMR spectrum (126 MHz, chloroform-*d*) of **4a**.

Sample Information

Sample Name	:
Tray#	: 1
Vial#	: 9
Injection Volume	: 10
Data File	: TE3.4-5,F11-17.lcd
Method File	: MSP5-95_30min_1.0.lcm
Batch File	: Batch-030921.lcb
Report Format File	: Reportformat1.lsr
Date Acquired	: 03.09.2021 11:15:36
Date Processed	: 03.09.2021 11:45:37

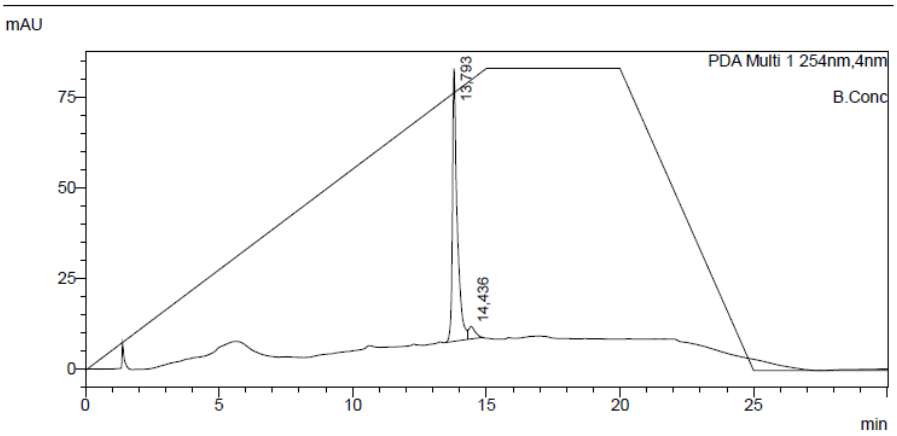

PDA Ch1 254nm

Peak#	Ret. Time	Area	Height	Area%
1	13,793	923580	75250	93,840
2	14,436	60631	3461	6,160
Total		984212	78710	100,000

Figure S3 HPLC trace of **4a**.

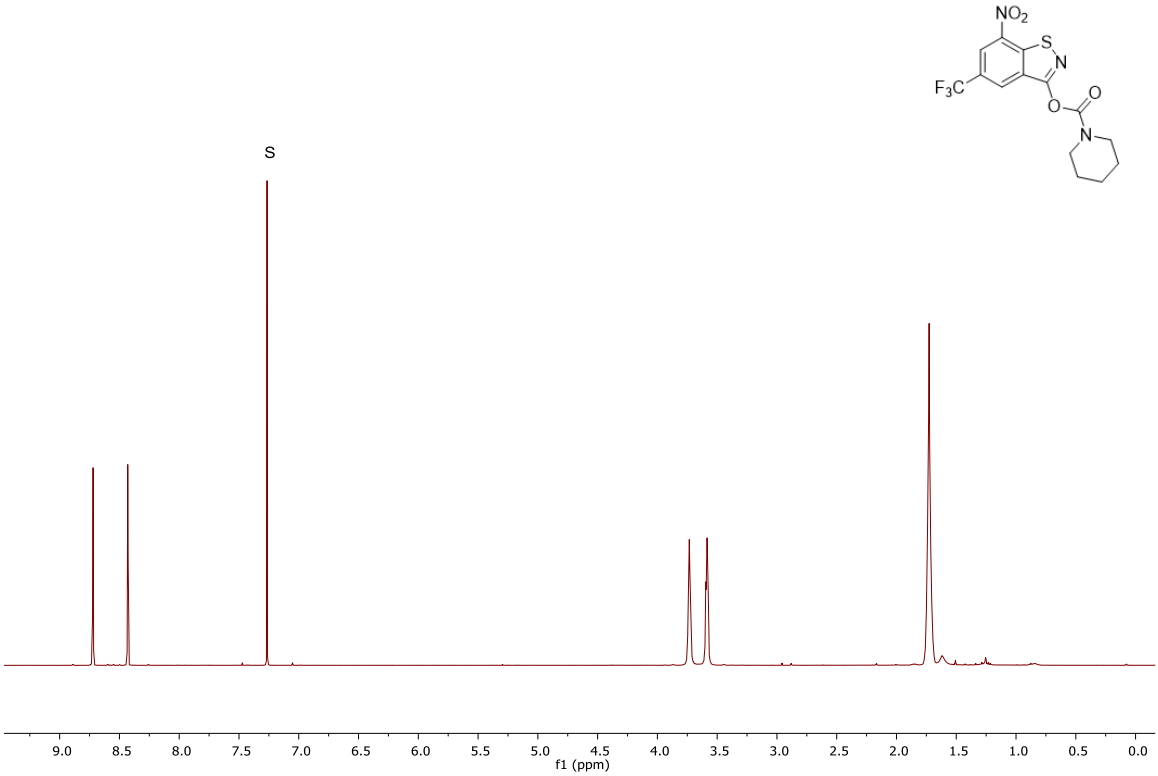

Figure S4 ^{1}H NMR spectrum (500 MHz, chloroform-*d*) of **5a**.

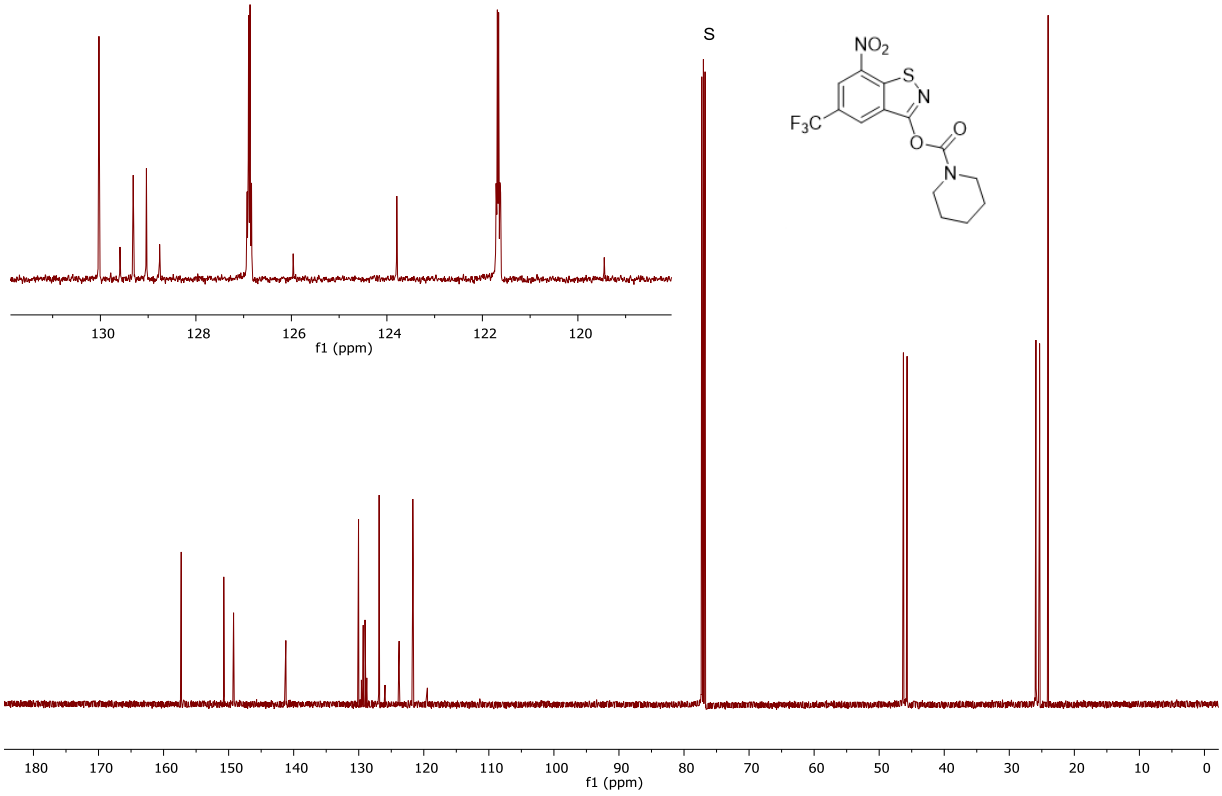

Figure S5 ^{13}C NMR spectrum (126 MHz, chloroform-*d*) of **5a**.

Sample Information

Sample Name	:
Tray#	: 1
Vial#	: 8
Injection Volume	: 10
Data File	: TE3.4-5,F4-6.lcd
Method File	: MSP5-95_30min_1.0.lcm
Batch File	: Batch-030921.lcb
Report Format File	: Reportformat1.lsr
Date Acquired	: 03.09.2021 10:45:08
Date Processed	: 03.09.2021 11:15:10

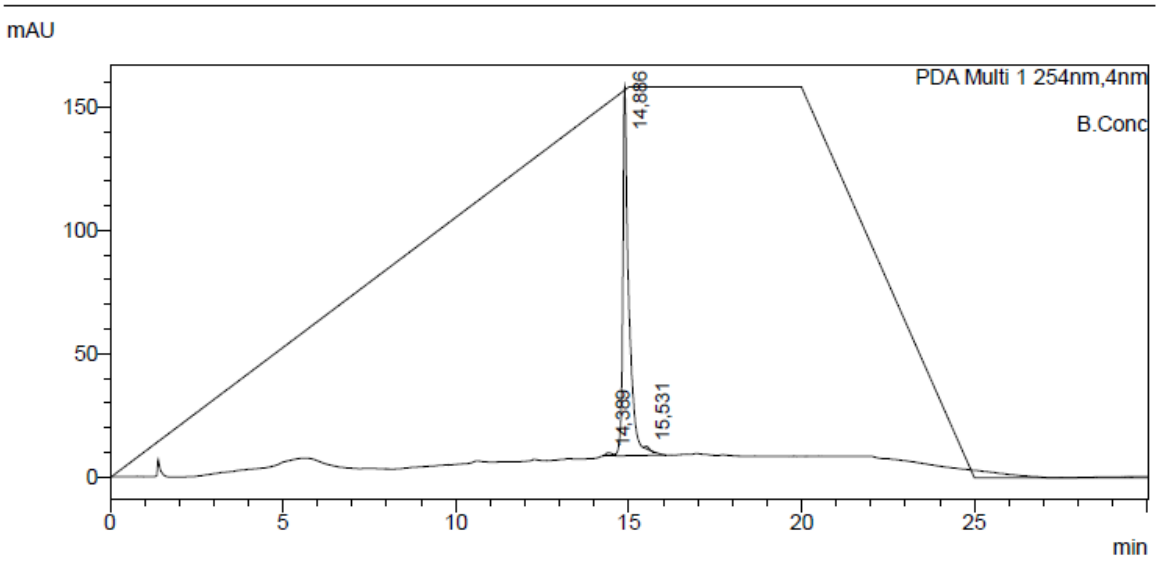

PDA Ch1 254nm

Peak#	Ret. Time	Area	Height	Area%
1	14,389	18558	1255	1,001
2	14,886	1827951	149596	98,594
3	15,531	7510	979	0,405
Total		1854019	151830	100,000

Figure S6 HPLC trace of **5a**.

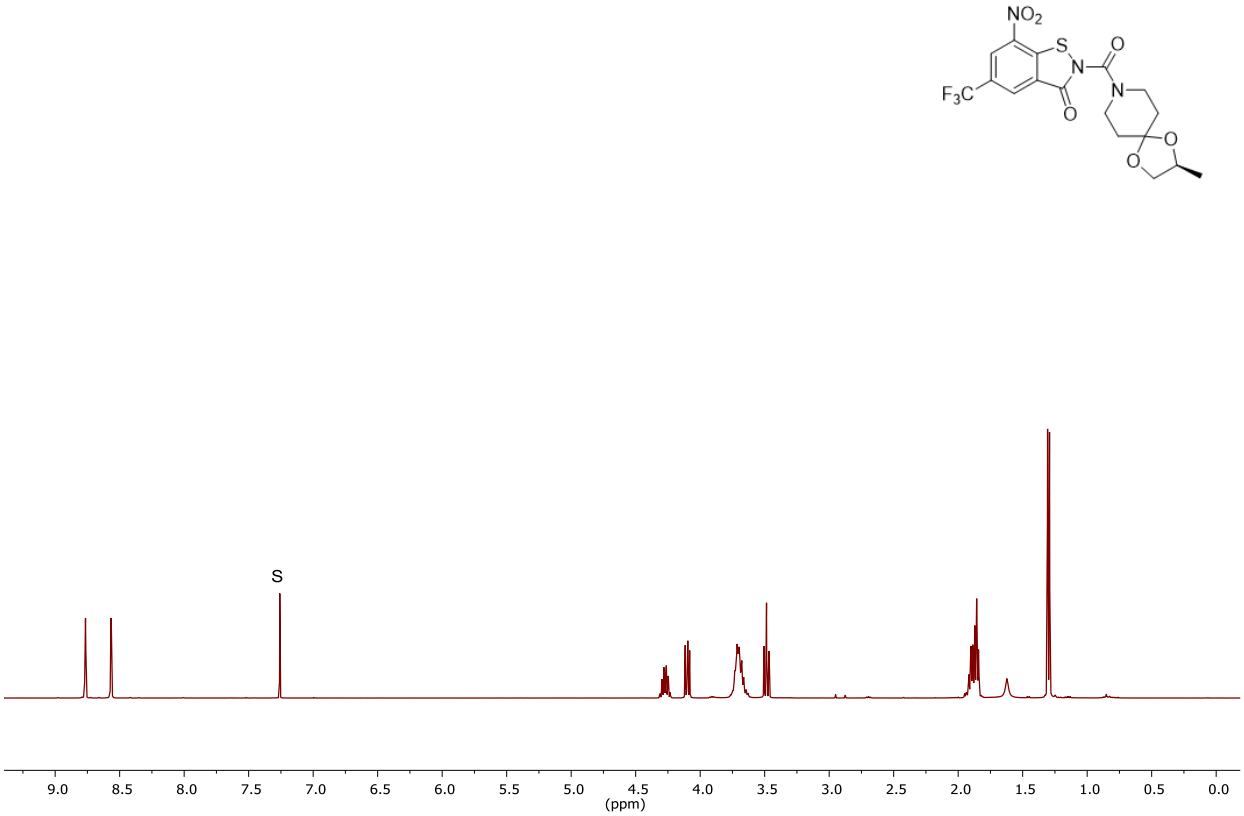

Figure S7 ^{1}H NMR spectrum (400 MHz, chloroform-*d*) of **4b**.

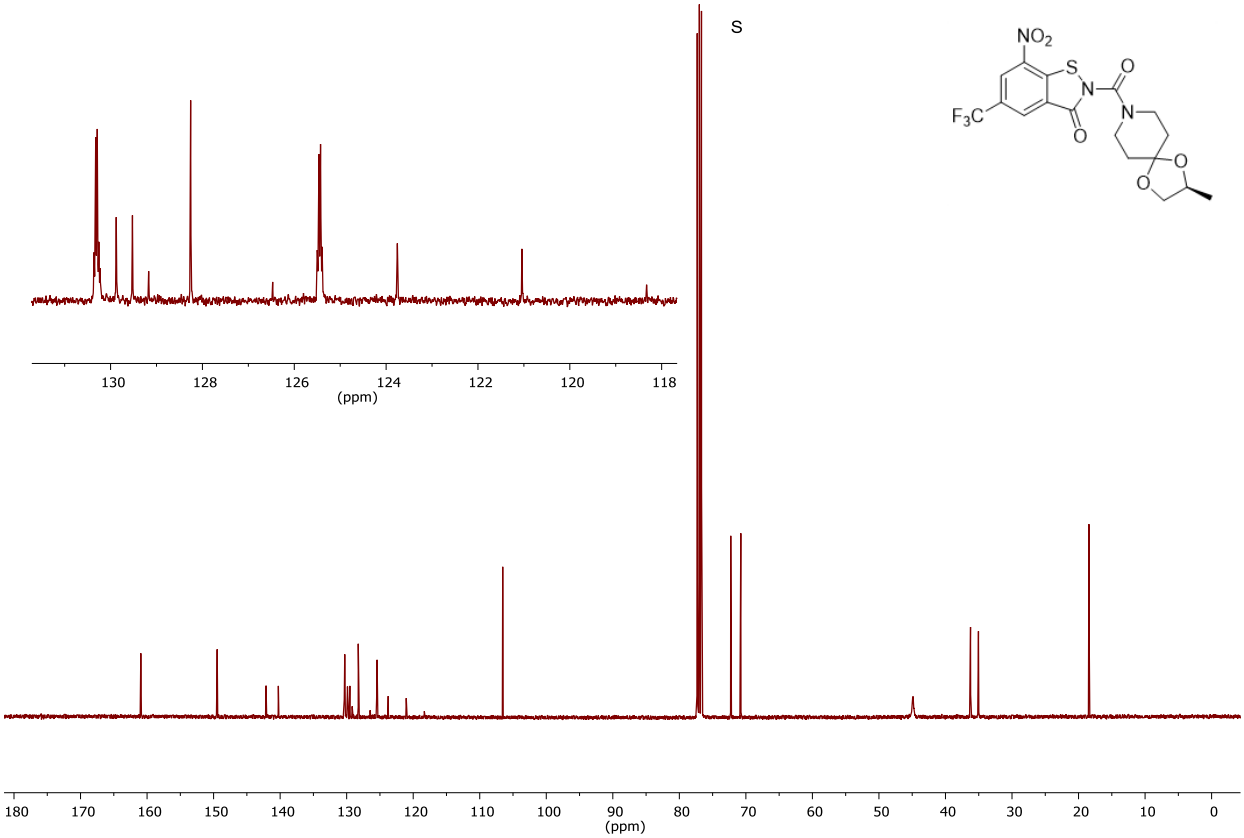

Figure S8 ^{13}C NMR spectrum (101 MHz, chloroform-*d*) of **4b**.

Sample Information

Sample Name	:
Tray#	: 1
Vial#	: 7
Injection Volume	: 10
Data File	: AR351,F10-14.lcd
Method File	: MSP5-95_30min_1.0.lcm
Batch File	: Batch-030921.lcb
Report Format File	: Reportformat1.lsr
Date Acquired	: 03.09.2021 10:14:38
Date Processed	: 03.09.2021 10:44:43

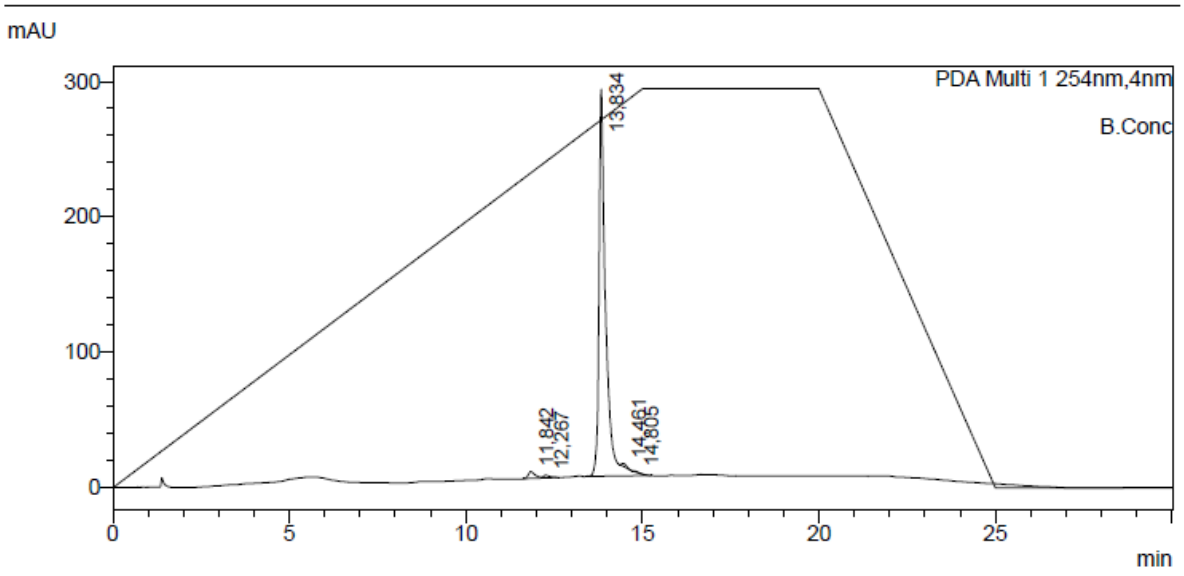

PDA Ch1 254nm

Peak#	Ret. Time	Area	Height	Area%
1	11,842	69588	5073	1,794
2	12,267	27367	2062	0,706
3	13,834	3757284	286136	96,889
4	14,461	19743	2172	0,509
5	14,805	3938	688	0,102
Total		3877920	296130	100,000

Figure S9 HPLC trace of **4b**.

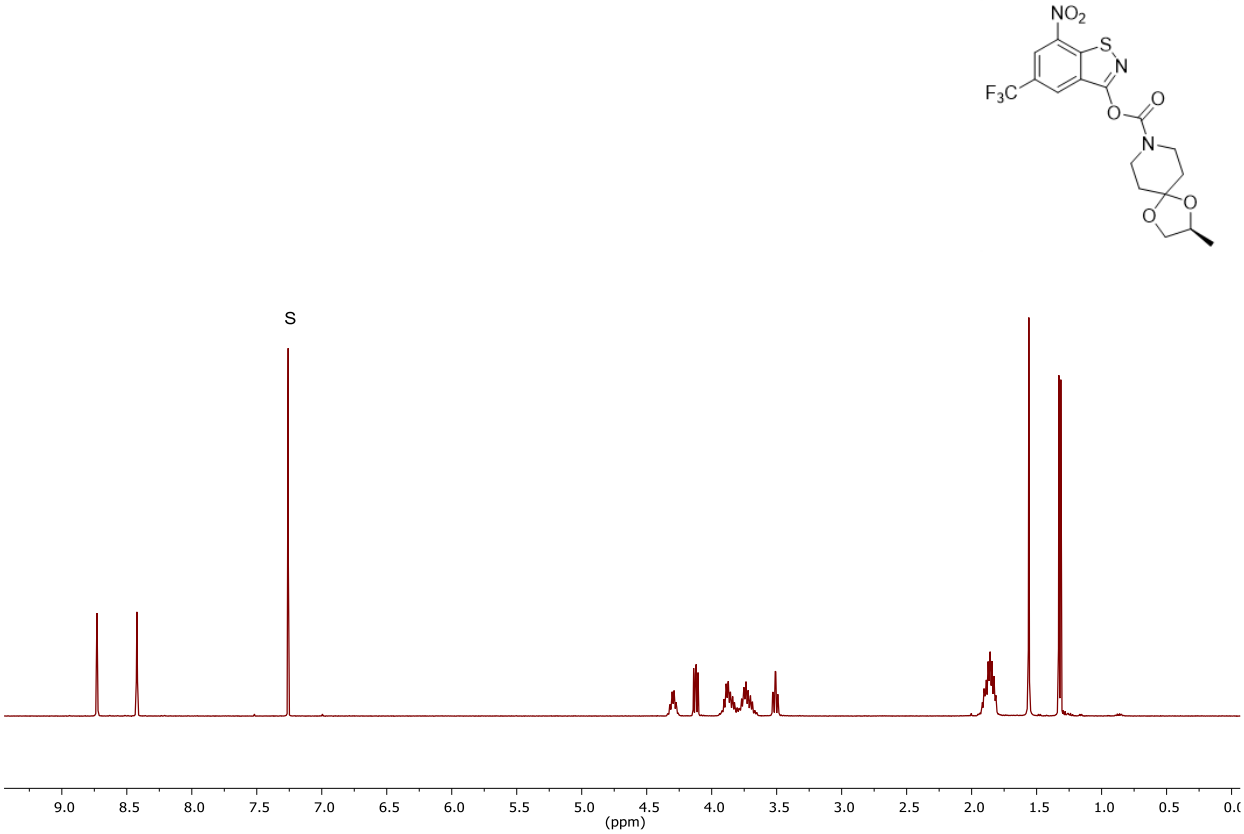

Figure S10 ^{1}H NMR spectrum (400 MHz, chloroform-*d*) of **5b**.

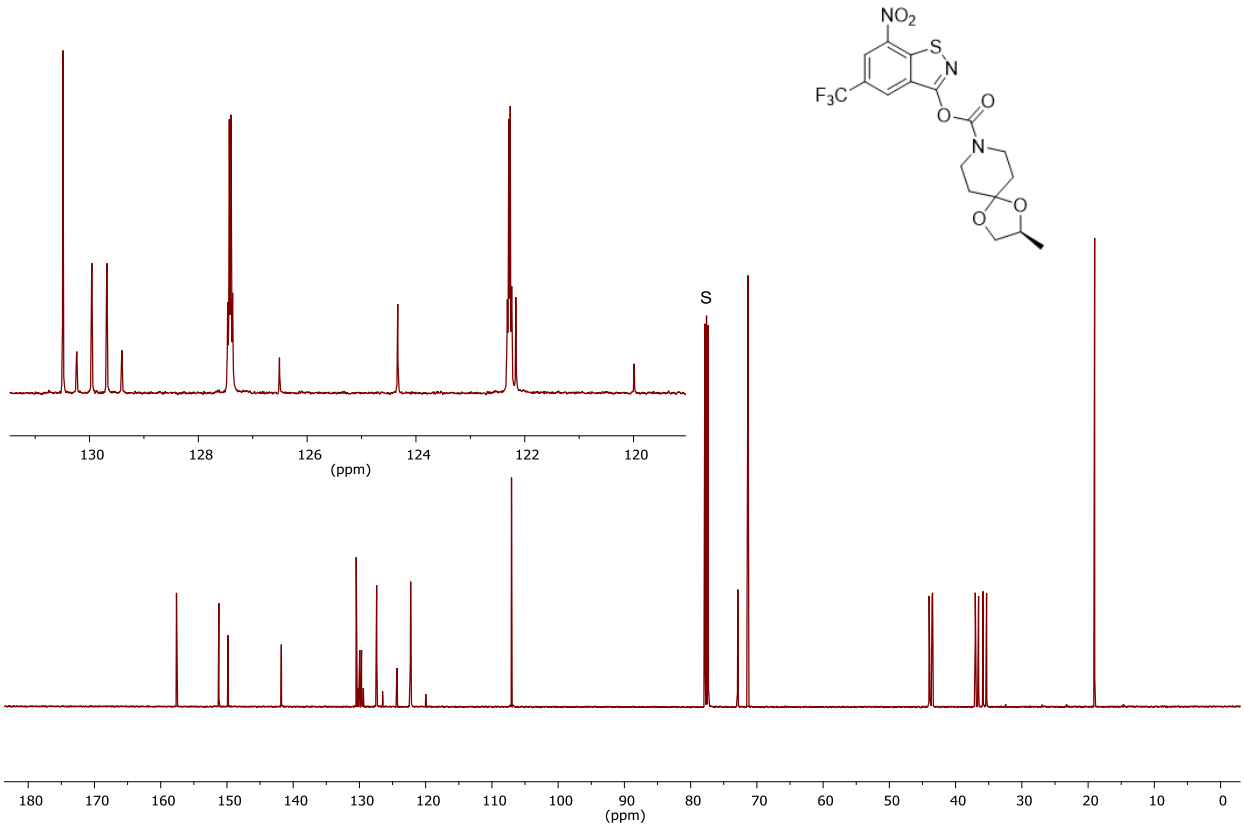

Figure S11 ^{13}C NMR spectrum (126 MHz, chloroform-*d*) of **5b**.

Sample Information

Sample Name	:
Tray#	: 1
Vial#	: 6
Injection Volume	: 10
Data File	: AR351,F1-5.lcd
Method File	: MSP5-95_30min_1.0.lcm
Batch File	: Batch-030921.lcb
Report Format File	: Reportformat1.lsr
Date Acquired	: 03.09.2021 09:44:11
Date Processed	: 03.09.2021 10:14:13

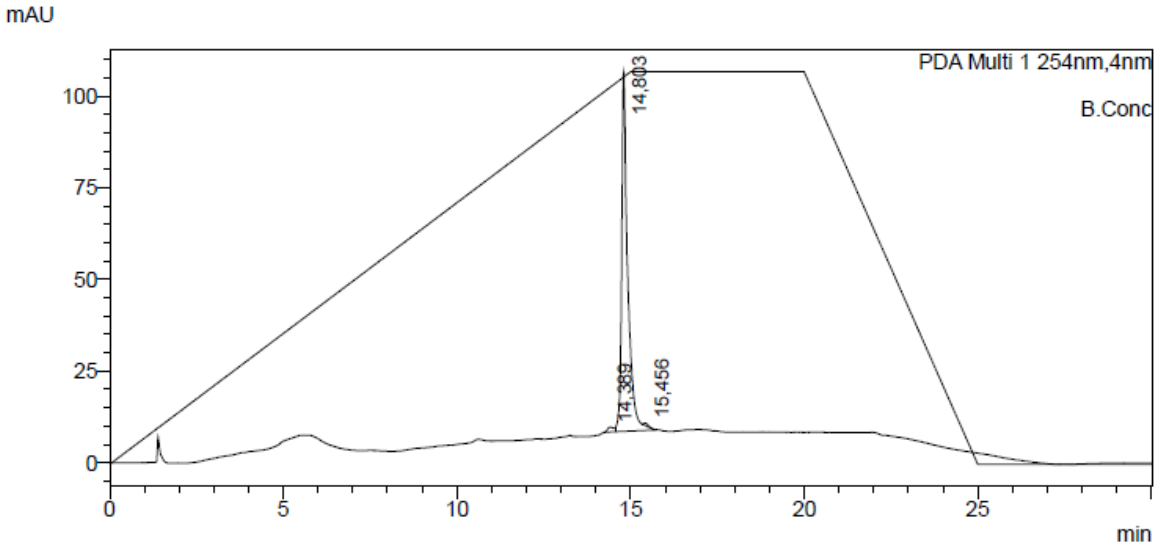

PDA Ch1 254nm

Peak#	Ret. Time	Area	Height	Area%
1	14,389	16621	1246	1,375
2	14,803	1187085	98017	98,177
3	15,456	5427	676	0,449
Total		1209133	99940	100,000

Figure S12 HPLC trace of **5b**.

4. X-ray crystallography

Crystals suitable for single-crystal X-ray diffraction were obtained from solutions of the compounds by slow diffusion of heptane into solutions of the compounds in chloroform and subsequent slow evaporation of the solvents. The X-ray intensity data for **4a** and **4b** were collected on a Bruker AXS Kappa Mach3 diffractometer equipped with an APEX II detector, a FR591 0.2 × 2 mm^2 focus rotating Cu anode X-ray source and Montel multilayer optics. The diffraction data for **5a** and **5b** were measured on a Bruker AXS Kappa Mach3 diffractometer with an APEX II detector and an Incoatec IμS microfocus Mo anode X-ray source. The data were processed using the SAINT[2] software. Numerical absorption corrections based on Gaussian integration over a multifaceted crystal model and scaling were carried out with SADABS.[3] The crystal structures were solved with SHELXT[4] and refined with SHELXL-2018/3.[5] For **5a**, the final structure refinement was carried out with Olex2[6] using aspherical scattering factors (NoSpherA2),[7] DFT-calculated with ORCA[8] using a B3LYP[9, 10] functional and def2-TZVPP basis set, whereby the H atom positions were refined using isotropic atomic displacement parameters.

In the structure refinement of **4a**, the occupancy of the water molecule was constrained to 0.75 and one water hydrogen atom was split over two disorder sites with equal occupancies. Split models were refined for rotational disorder of trifluoromethyl groups in **4a** and **5b**, using standard similar distance restraints on 1,2- and 1,3-distances as well as rigid bond restraints[11] and restraints towards isotropy on anisotropic atomic displacement parameters. The ratios of occupancies were refined by means of free variables. The absolute structure of **4b** and **5b** was inferred from the known *S*-configuration at the chirality center in the methyldioxolan moiety and confirmed by a Flack *x* parameter close to zero,[12] using Parsons' method.[13] Structure pictures were drawn with Mercury.[14]

Computational methods

DFT calculations were undertaken using the program ORCA (version 5.0)[8] with a B3LYP/G VWN1 hybrid functional (20% HF exchange),[9, 10, 15] using a def2-TZVPP basis set.[16] Optimization of the structures used the BFGS method from an initial Hessian according to Almoef's model with a very tight self-consistent field convergence threshold.[17] Calculations were made on the free molecules. The optimized local minimum-energy structures exhibited only positive modes. Natural charges were calculated by natural bond orbital analysis using the program NBO 7.0.0.[18] The wave function was converted from the standard ORCA-file format (.gbw) to the Molden format with the ORCA routine *orca_2mkl*. Subsequently, the electrostatic

potential (ESP) and the electron density were generated from this file using the program Multiwfn 3.6 and both quantities were written in the Gaussian cube file format.[19] The calculated ESP was mapped onto the electron density isosurface with the value 0.001 a.u. using the visualization program VMD 1.9.3.[20] Molden 5.0[21] and Avogadro 1.2.0[22] were used as model editor and visualization tools.

5. Computational methods

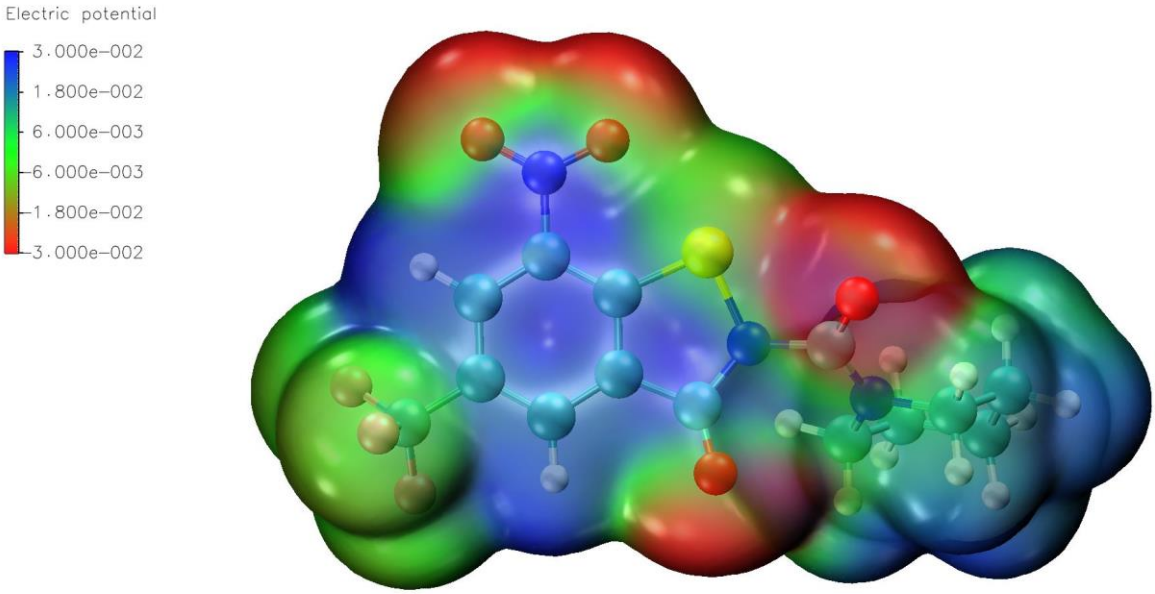

Figure S13 DFT-optimized molecular structure of **4a** and the electrostatic potential mapped onto the 0.001 eÅ^{-3} electron density isosurface (a.u.).

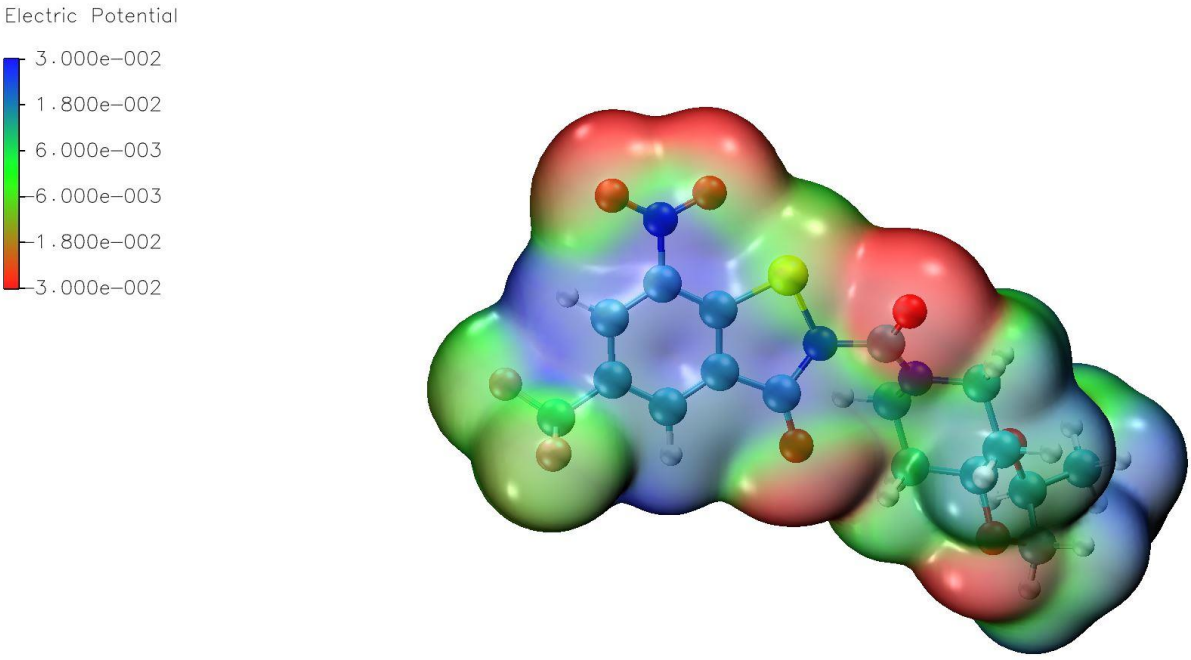

Figure S14 DFT-optimized molecular structure of **4b** with the electrostatic potential mapped onto the 0.001 eÅ^{-3} electron density isosurface (a.u.).

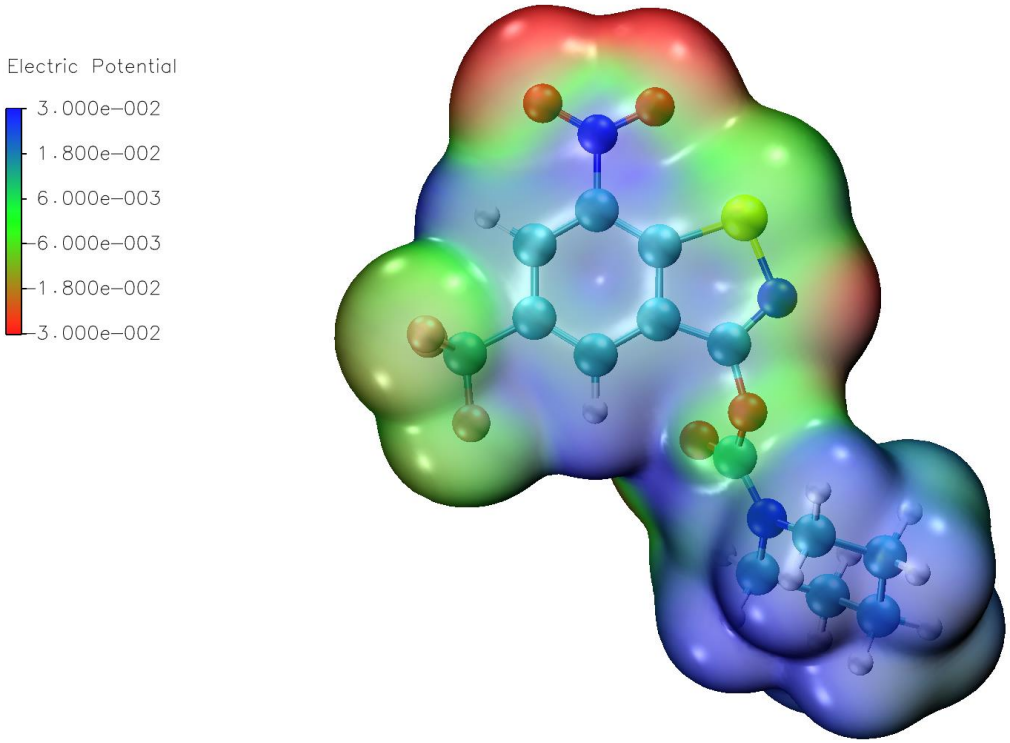

Figure S15 DFT-optimized molecular structure of **5a** with the electrostatic potential mapped onto the 0.001 eÅ^{-3} electron density isosurface (a.u.).

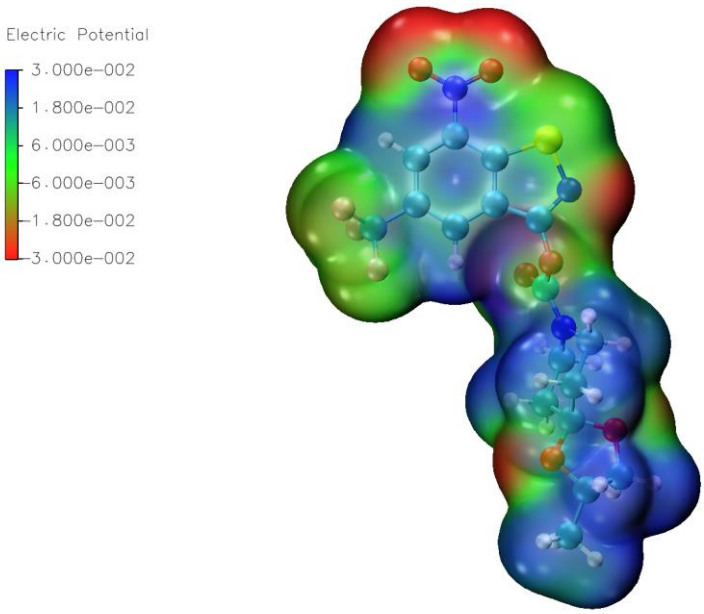

Figure S16 DFT-optimized molecular structure of **5b** with the electrostatic potential mapped onto the 0.001 eÅ^{-3} electron density isosurface (a.u.).

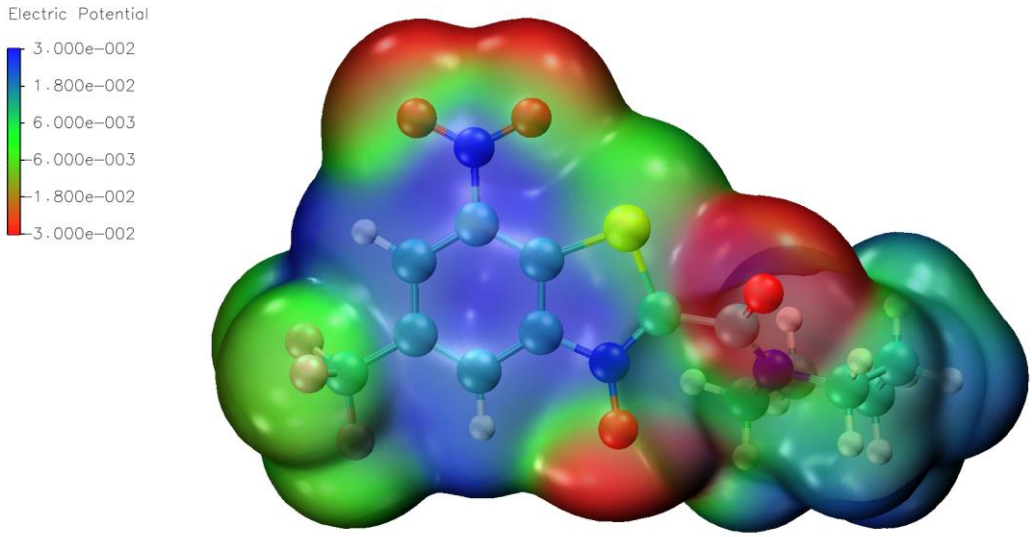

Figure S17 DFT-optimized molecular structure of **6a** with the electrostatic potential mapped onto the 0.001 eÅ^{-3} electron density isosurface (a.u.).

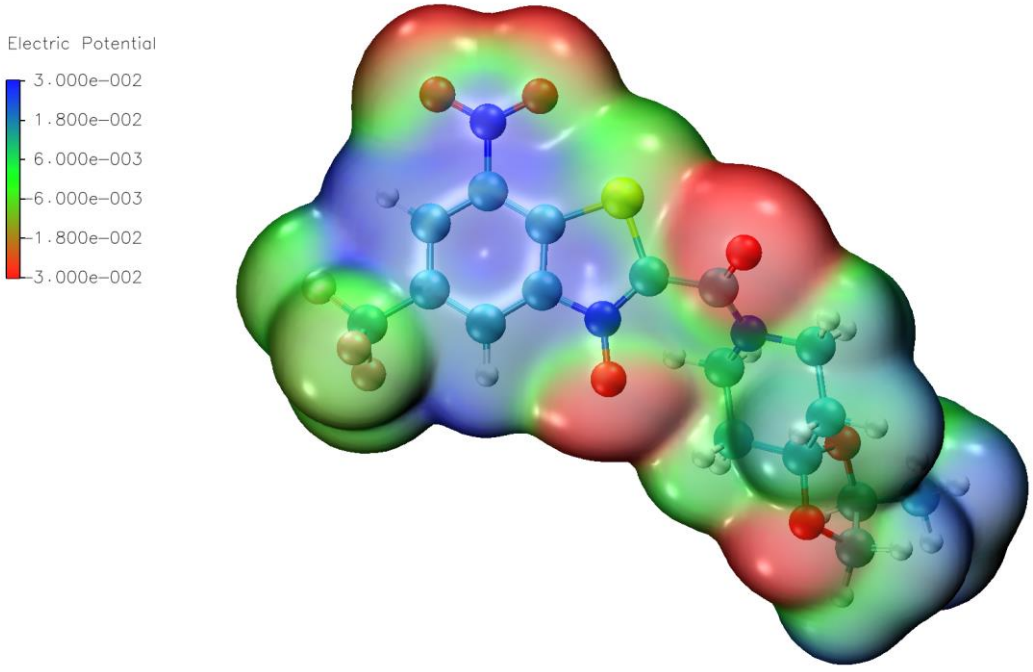

Figure S18 DFT-optimized molecular structure of **6b** with the electrostatic potential mapped onto the 0.001 eÅ^{-3} electron density isosurface (a.u.).

6. Antimycobacterial evaluation

Mtb growth analysis in liquid culture

M. tuberculosis (Mtb) strain H37Rv (ATCC 25618) carrying a mCherry-expressing plasmid (pCherry10)[23] was cultured in 7H9 complete medium (BD Difco; Becton Dickinson) supplemented with oleic acid-albumin-dextrose-catalase (OADC, 10%; BD), 0.2% glycerol, and 0.05 % polysorbate 80 as previously described. At mid-log phase (OD600 = 0.4) cultures were harvested and frozen in aliquots at −80 °C.[24]

Frozen aliquots of mCherry-Mtb H37Rv were thawed and centrifuged (3700×g, 10 minutes). Supernatants were discarded and bacteria thoroughly resuspended in 7H9 medium (10% OADC) in the absence of glycerol and Tween80 by use of a syringe and a 26-gauge syringe needle. The bacterial suspension was passed in and out of the syringe about 10 times. Compounds were tested in 2 fold dilutions starting at 64 µM in triplicates (2×10e6 bacteria, volume 100 µl) for their anti-tubercular activity using 96-well flat clear bottom black polystyrene microplates (Corning® CellBIND®, New York, USA). Each plate was prepared with rifampicin (National Reference Center, Borstel) as reference compound. Plates were sealed with an air-permeable membrane (Porvair Sciences, Wrexham, UK) in a 37◦C incubator with mild agitation (TiMix5, Edmund Bühler, Germany), as previously described[25]. Bacterial growth was measured as relative light units (RLU) from the fluorescence intensity obtained at an excitation wavelength of 575 nm and emission wavelength of 635 nm (microplate reader, Synergy 2, BioTek Instruments, Vermont, USA) at the indicated time points. Obtained values were normalized to RLU values of the solvent control (DMSO)-treated bacteria set to 100%) and MIC95 of each compound was determined. MIC95 was defined as the minimum concentration of the compound required to achieve a reduction in fluorescence by 95%. Obtained MIC values were validated by a visual Resazurin microtiter assay (REMA)[26] by adding 30 µL of 0,02% Resazurin (Cayman) solution to each well followed by another 20 h of culture without agitation.

M. smegmatis and M. aurum growth analysis in liquid culture

MIC determination against *M. smegmatis* mc² 155 pTEC27 and *M. aurum* DSM43999. MICs were determined by the broth microdilution method. 96-well flat bottom tissue culture plates (Sarstedt, 83.3924.500) were used.[27] In the second well of each row two times of the desired highest concentration of each compound was added in 7H9 medium supplemented with 10 % ADS and 0.05 % polysorbate 80. Each compound was diluted twofold in a ten-point serial

dilution. The concentration of the starting inoculum was 5×10^5 cells/mL. The starting inoculum was diluted from a preculture at the mid-log phase (OD_{600} 0.3 to 0.7) and an OD_{600} of 0.1 was correlated to 1×10^8 CFU/mL. The plates were sealed with parafilm, placed in a container with moist tissue and incubated for four days at 37 °C. Each plate had eight negative controls (1 % dimethylsulfoxide) and eight positive controls (100 µM amikacin). After incubation the plates were monitored by OD measurement at 590 nm (Tecan SpectraFluor). The assay was performed in duplicate and results were validated by RFP measurement for *M. smegmatis* pTec27.

Data analysis: Every assay plate contained eight wells with dimethylsulfoxide (1 %) as negative control, which corresponds to 100 % bacterial growth and eight wells with amikacin (100 µM) as positive control in which 100 % inhibition of bacterial growth was reached. Controls were used to monitor the assay quality through determination of the Z' score. The Z' factor was calculated as follows:

$$(1)\ Z' = 1 - \frac{3(\mathrm{SD}_{\mathrm{amikacin}} + \mathrm{SD}_{\mathrm{DMSO}})}{\mathrm{M}_{\mathrm{amikacin}} - \mathrm{M}_{\mathrm{DMSO}}}$$

(SD = standard deviation, M = mean)

The percentage of growth inhibition was calculated by the equation:

$$(2)\ \%\ \text{growth inhibition} = -100\ \% \times \frac{\mathrm{OD}_{590}(\mathrm{sample}) - \mathrm{OD}_{590}(\mathrm{DMSO})}{\mathrm{OD}_{590}(\mathrm{DMSO}) - \mathrm{OD}_{590}(\mathrm{amikacin})}$$

7. Molecular Docking

Docking experiments were performed with Gold (2021.2).[28] The crystal structure of BTZ043 in complex with *M. tuberculosis* DprE1 (PDB ID: 6HEZ)[29] was obtained from the Protein Data bank.[30] From this, chain B, B.FAD and crystal waters were extracted and prepared for the molecular docking processes, using MOE (2020.0901).[31] A special feature of the dockings was a previously defined covalent bond of all ligands to cysteine 387. To implement this, the atom type of the ligand atom to be linked, was labelled appropriately. The initial evaluation of the docking solutions was accomplished with the scoring function GoldScore. Subsequently, the solutions obtained were rescored using ChemScore. 30 docking runs were performed with early termination. The docking site was defined within an 20Å sphere around SG,C387 atom. Furthermore, five amino acid side chains of the binding site were flexibly considered to optimize the placement for the new ligands. This flexibility was realized by rotamer libraries for K134, W230, V365, L363 and K418. Initially, the binding mode of co-crystallized compound **1b** was confirmed.

All *in silico* methods used were able to replace the compound with a very high precision (Figure S19). The docking pose corresponds to the orientation of **1b** encountered in the crystal structure in complex with the *M. tuberculosis* DprE1,[29] which also shows the invariant trifluoromethyl group in the direction Lys134, Gly133, His132, Lys367 and Phe369.

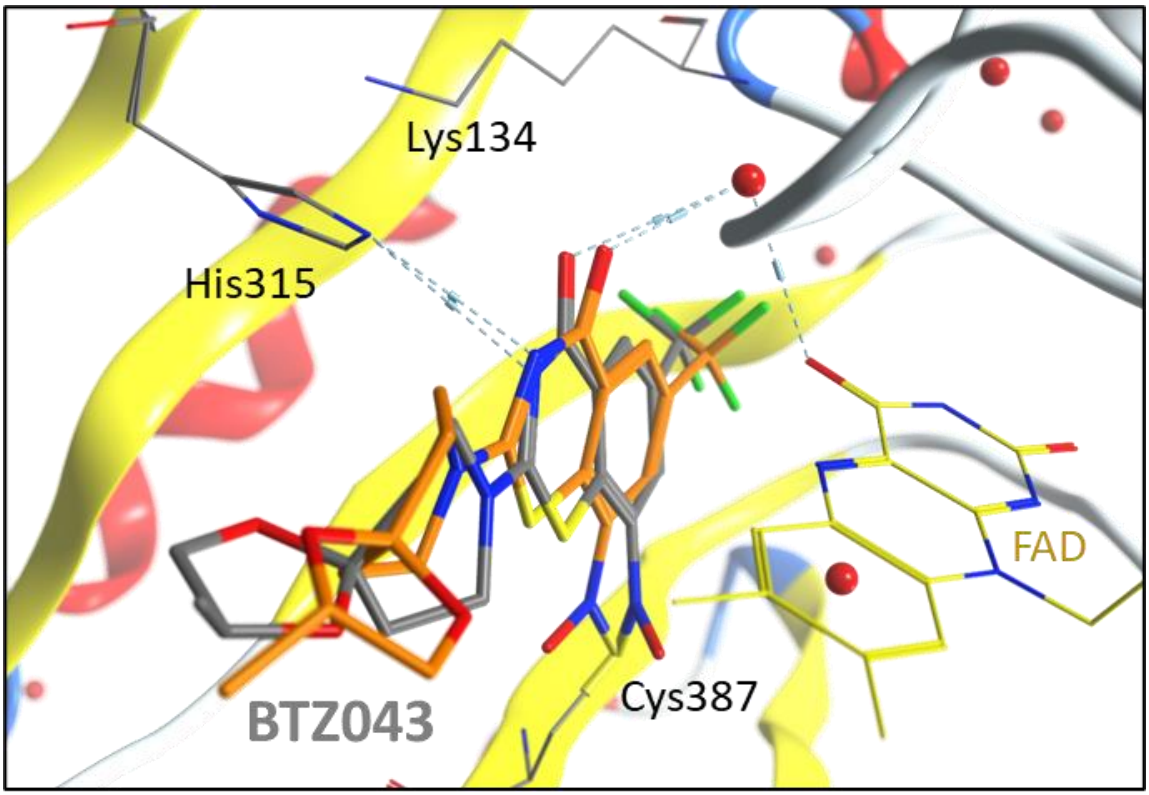

Figure S19 Proof of concept: structure overlay plot of **1b** (BTZ043) in complex with *M. tuberculosis* DprE1 (PDB ID: 6HEZ) [29] (grey) and docking pose (orange).

Table S1 Total fitness scores, number count and calculated ranges of all docking solutions.

	Solution count	total scoring range (GoldScore fitness)	total scoring range [rescore] (ChemScore fitness)
4a	5	30.7684–24.3232	23.3178 – 19.9778
4b	5	23.6796–18.3279	26.3235 – 22.0269
5a	6	4.8693–0.0000	18.1415 – (–66.0295)
5b	21	7.6315–(–1.3696)	23.8707 – (–62.1347)

Table S2 Molecular docking solutions used for further analysis and pictures (see Figure 8).

	Solution number	GoldScore fitness	ChemScore fitness
4a	5	30.7684	21.7778
4b	2	23.6796	22.0269
5a	5	4.8693	16.2341
5b	15	7.6315	19.953

8. References

1. Richter, A.; Goddard, R.; Schlegel, T.; Imming, P.; Seidel, R. W., 2-Chloro-3-nitro-5-(trifluoromethyl)benzoic acid and -benzamide: structural characterization of two precursors for antitubercular benzothiazinones. *Acta Crystallographica Section E* **2021,** *77* (2), 142-147.
2. *SAINT*, Bruker AXS Inc.: Madison, Wisconsin, USA, 2012.
3. *SADABS*, Bruker AXS Inc.: Madison, Wisconsin, USA, 2012.
4. Sheldrick, G. M., SHELXT - integrated space-group and crystal-structure determination. *Acta Crystallogr A Found Adv* **2015,** *71* (Pt 1), 3-8.
5. Sheldrick, G. M., Crystal structure refinement with SHELXL. *Acta Crystallogr C Struct Chem* **2015,** *71* (Pt 1), 3-8.
6. Bourhis, L. J.; Dolomanov, O. V.; Gildea, R. J.; Howard, J. A. K.; Puschmann, H., The anatomy of a comprehensive constrained, restrained refinement program for the modern computing environment - Olex2 dissected. *Acta Crystallographica Section A* **2015,** *71* (1), 59-75.
7. Kleemiss, F.; Dolomanov, O. V.; Bodensteiner, M.; Peyerimhoff, N.; Midgley, L.; Bourhis, L. J.; Genoni, A.; Malaspina, L. A.; Jayatilaka, D.; Spencer, J. L.; White, F.; Grundkötter-Stock, B.; Steinhauer, S.; Lentz, D.; Puschmann, H.; Grabowsky, S., Accurate crystal structures and chemical properties from NoSpherA2. *Chemical Science* **2021,** *12* (5), 1675-1692.
8. Neese, F., Software update: the ORCA program system, version 4.0. *WIREs Computational Molecular Science* **2018,** *8* (1), e1327.
9. Becke, A. D., Density-functional thermochemistry. III. The role of exact exchange. *The Journal of Chemical Physics* **1993,** *98* (7), 5648-5652.
10. Lee, C.; Yang, W.; Parr, R. G., Development of the Colle-Salvetti correlation-energy formula into a functional of the electron density. *Physical Review B* **1988,** *37* (2), 785-789.
11. Thorn, A.; Dittrich, B.; Sheldrick, G. M., Enhanced rigid-bond restraints. *Acta Crystallographica Section A* **2012,** *68* (4), 448-451.
12. Flack, H., On enantiomorph-polarity estimation. *Acta Crystallographica Section A* **1983,** *39* (6), 876-881.
13. Parsons, S.; Flack, H. D.; Wagner, T., Use of intensity quotients and differences in absolute structure refinement. *Acta Crystallogr B Struct Sci Cryst Eng Mater* **2013,** *69* (Pt 3), 249-59.
14. Macrae, C. F.; Sovago, I.; Cottrell, S. J.; Galek, P. T. A.; McCabe, P.; Pidcock, E.; Platings, M.; Shields, G. P.; Stevens, J. S.; Towler, M.; Wood, P. A., Mercury 4.0: from visualization to analysis, design and prediction. *J Appl Crystallogr* **2020,** *53* (Pt 1), 226-235.
15. Hertwig, R. H.; Koch, W., On the parameterization of the local correlation functional. What is Becke-3-LYP? *Chem. Phys. Lett.* **1997,** *268* (5), 345-351.
16. Weigend, F.; Ahlrichs, R., Balanced basis sets of split valence, triple zeta valence and quadruple zeta valence quality for H to Rn: Design and assessment of accuracy. *Physical Chemistry Chemical Physics* **2005,** *7* (18), 3297-3305.
17. Fletcher, R., *Practical Methods of Optimization, 2nd Edition*. 2nd ed ed.; John Wiley & Sons: 2000.
18. E. D. Glendening, J., K. Badenhoop, A. E. Reed, J. E. Carpenter, J. A. Bohmann, C. M. Morales, P. Karafiloglou, C. R. Landis, F. Weinhold *NBO 7.0*, Theoretical Chemistry Institute, University of Wisconsin: Madison, Wisconsin, USA, 2018.
19. Lu, T.; Chen, F., Multiwfn: A multifunctional wavefunction analyzer. *Journal of Computational Chemistry* **2012,** *33* (5), 580-592.
20. Humphrey, W.; Dalke, A.; Schulten, K., VMD: Visual molecular dynamics. *Journal of Molecular Graphics* **1996,** *14* (1), 33-38.
21. Schaftenaar, G.; Noordik, J. H., Molden: a pre- and post-processing program for molecular and electronic structures*. *Journal of Computer-Aided Molecular Design* **2000,** *14* (2), 123-134.
22. Hanwell, M. D.; Curtis, D. E.; Lonie, D. C.; Vandermeersch, T.; Zurek, E.; Hutchison, G. R., Avogadro: an advanced semantic chemical editor, visualization, and analysis platform. *Journal of Cheminformatics* **2012,** *4* (1), 17.

23. Zelmer, A.; Carroll, P.; Andreu, N.; Hagens, K.; Mahlo, J.; Redinger, N.; Robertson, B. D.; Wiles, S.; Ward, T. H.; Parish, T.; Ripoll, J.; Bancroft, G. J.; Schaible, U. E., A new in vivo model to test anti-tuberculosis drugs using fluorescence imaging. *J. Antimicrob. Chemother.* **2012,** *67* (8), 1948-60.
24. Kolbe, K.; Mockl, L.; Sohst, V.; Brandenburg, J.; Engel, R.; Malm, S.; Brauchle, C.; Holst, O.; Lindhorst, T. K.; Reiling, N., Azido Pentoses: A New Tool To Efficiently Label Mycobacterium tuberculosis Clinical Isolates. *Chembiochem* **2017,** *18* (13), 1172-1176.
25. Jumde, R. P.; Guardigni, M.; Gierse, R. M.; Alhayek, A.; Zhu, D.; Hamid, Z.; Johannsen, S.; Elgaher, W. A. M.; Neusens, P. J.; Nehls, C.; Haupenthal, J.; Reiling, N.; Hirsch, A. K. H., Hit-optimization using target-directed dynamic combinatorial chemistry: development of inhibitors of the anti-infective target 1-deoxy-d-xylulose-5-phosphate synthase. *Chem Sci* **2021,** *12* (22), 7775-7785.
26. Franzblau, S. G.; DeGroote, M. A.; Cho, S. H.; Andries, K.; Nuermberger, E.; Orme, I. M.; Mdluli, K.; Angulo-Barturen, I.; Dick, T.; Dartois, V.; Lenaerts, A. J., Comprehensive analysis of methods used for the evaluation of compounds against Mycobacterium tuberculosis. *Tuberculosis (Edinb)* **2012,** *92* (6), 453-88.
27. Richter, A.; Strauch, A.; Chao, J.; Ko, M.; Av-Gay, Y., Screening of Preselected Libraries Targeting Mycobacterium abscessus for Drug Discovery. *Antimicrobial Agents and Chemotherapy* **2018,** *62* (9), e00828-18.
28. Jones, G.; Willett, P.; Glen, R. C.; Leach, A. R.; Taylor, R., Development and validation of a genetic algorithm for flexible docking11Edited by F. E. Cohen. *J. Mol. Biol.* **1997,** *267* (3), 727-748.
29. Richter, A.; Rudolph, I.; Möllmann, U.; Voigt, K.; Chung, C.-w.; Singh, O. M. P.; Rees, M.; Mendoza-Losana, A.; Bates, R.; Ballell, L.; Batt, S.; Veerapen, N.; Fütterer, K.; Besra, G.; Imming, P.; Argyrou, A., Novel insight into the reaction of nitro, nitroso and hydroxylamino benzothiazinones and of benzoxacinones with Mycobacterium tuberculosis DprE1. *Scientific Reports* **2018,** *8* (1), 13473.
30. Burley, S. K.; Berman, H. M.; Bhikadiya, C.; Bi, C.; Chen, L.; Di Costanzo, L.; Christie, C.; Dalenberg, K.; Duarte, J. M.; Dutta, S.; Feng, Z.; Ghosh, S.; Goodsell, D. S.; Green, R. K.; Guranovic, V.; Guzenko, D.; Hudson, B. P.; Kalro, T.; Liang, Y.; Lowe, R.; Namkoong, H.; Peisach, E.; Periskova, I.; Prlic, A.; Randle, C.; Rose, A.; Rose, P.; Sala, R.; Sekharan, M.; Shao, C.; Tan, L.; Tao, Y. P.; Valasatava, Y.; Voigt, M.; Westbrook, J.; Woo, J.; Yang, H.; Young, J.; Zhuravleva, M.; Zardecki, C., RCSB Protein Data Bank: biological macromolecular structures enabling research and education in fundamental biology, biomedicine, biotechnology and energy. *Nucleic Acids Res* **2019,** *47* (D1), D464-D474.
31. *Molecular Operating Environment (MOE)*, 2020.09; Chemical Computing Group ULC: 1010 Sherbooke St. West, Suite #910, Montreal, QC, Canada, H3A 2R7, 2022.